Journal of Inorganic and General Chemistry
ZAAC
Zeitschrift für anorganische und allgemeine Chemie
DOI: 10.1002/zaac.202000265
ARTICLE

Ambient Temperature Synthesis and Structural Characterization of Six Transition Metal Acetylenedicarboxylate Coordination Polymers

Luke Best-Thompson[a] and Paul J. Saines*[a]

Abstract. This work reports the ambient temperature synthesis and structural characterization of six new first row transition metal acetylenedicarboxylate coordination polymers. The Co and two Ni compounds adopt structures in which the octahedral metals are connected into 1D chains via the acetylenedicarboxylate ligand. In contrast the Mn and two Zn compounds adopt 3D metal-organic frameworks; while the Mn compound is non-porous the two Zn structures contain dimeric or trimeric clusters connected into frameworks that are potentially porous. These two anionic metal-organic frameworks are, however, charged balanced by cations siting in their pores which greatly reduces the ability to access their porosity.

Introduction

Metal-organic frameworks (MOFs) are structures comprised of inorganic nodes connected via organic linkers to form two or three dimensional structures, which are often potentially porous although debate remains on the essential nature of this.[1–3] As such they are a subcategory of coordination polymers incorporating organic ligands into higher dimensional structures. MOFs have attracted significant attention for the wide range of fascinating properties they can exhibit that are enhanced by the great flexibility in the range of building blocks they can incorporate and the fascinating range of structures that can result from this.[4–8] Despite many archetypical MOFs being built from dicarboxylates arguably one of the simplest of these, acetylenedicarboxylate, has been largely overlooked.[9–14] This is despite indications that frameworks containing such ligands would be expected to have particularly strong magnetic properties amongst coordination polymers[15] and would have potential for the use in capture and storage of halogen gases via chemisorption through reacting with the high density of alkyne groups they contain.[16–18]

Arguably the lack of acetylenedicarboxylate frameworks in the literature is due to the high reactivity and thermal lability of this ligand, which renders making such materials by solvothermal synthesis, as is commonly employed for MOFs, extremely challenging.[9,19] This is particularly the case for transition metal-based compounds, the most common inorganic building blocks in MOFs. There are, however, a significant number of first row transition metal coordination polymers made using this ligand by ambient temperature reactions, most commonly in water.[20–27] Similarly, the two known first row transition metal MOFs incorporating only acetylenedicarboxylate organic linkers were made at ambient temperature.[10,11] Thus it can be anticipated that a careful exploration of more gentle synthetic conditions in a range of simple organic solvents and employing a range of transition metals may lead to the discovery of new MOFs and coordination frameworks incorporating this ligand.

Given the potential for significant interest in acetylene-based coordination polymers and MOFs this study set out to establish the range of structures of such materials that could be made using alcohol solvents either through liquid or vapor diffusion methods, which commonly yield single crystals under ambient temperatures. This resulted in the discovery of six new coordination polymers, with compounds under these conditions containing Co and Ni found to form 1D coordination polymers while a Mn and two Zn phases form 3D MOFs. Of these the two Zn phases, which feature distinct inorganic clusters connected into three dimensional frameworks, are potentially porous. These are, however, occupied by counterions, primarily protonated base used in their synthesis, which are required to counterbalance the anionic frameworks. Significant problems, were however, encountered in isolating these in bulk form most likely due to their instability to solvent loss.

Results and Discussions

Synthesis and Crystal Structures

Extensive work was initially carried out to create transition metal acetylenedicarboxylate frameworks using vapor diffusion techniques. This involved the diffusion of a relative bulky amine base, most commonly *N*,*N*'-diisopropylethylamine, also known as Hunig's base (HUN), into a solution of

* Dr. P. J. Saines
E-mail: P.Saines@kent.ac.uk
[a] School of Physical Sciences, Ingram Building
University of Kent
Canterbury, Kent, CT2 7NH, United Kingdom
Supporting information for this article is available on the WWW under **http://dx.doi.org/10.1002/zaac.202000265** or from the author.

Table 1. Crystallographic details for the structures determined in this work.

	MnADC	CoADC	NiADC1	NiADC2	ZnADC1	ZnADC2
Formula	$Mn_2C_{13}H_{20}O_{13}$	$CoC_8H_{16}O_8$	$NiC_{11}H_{20}O_8$	$NiC_{12}H_{23}O_8$	$Zn_2C_{36}H_{60}\ N_4O_{15}$	$Zn_3C_{32}H_{40}\ N_2O_{16}$
Formula weight	494.17	299.14	338.98	354.01	919.62	904.77
T /K	292(2)	292(2)	293(2)	293(2)	100(2)	100(2)
λ /Å	1.54184	0.71073	1.54184	1.54184	1.54184	1.54184
Crystal system	monoclinic	monoclinic	monoclinic	triclinic	orthorhombic	orthorhombic
Space group	*C*2/*c*	*C*2/*c*	$P2_1/n$	$P\bar{1}$	$Pna2_1$	*Pbca*
a /Å	10.8875(8)	12.451(5)	9.6723(5)	9.3478(12)	18.1647(3)	20.7992(8)
b /Å	14.8481(14)	7.088(2)	16.1469(17)	9.6770(7)	15.6263(2)	15.2528(12)
c /Å	25.717(2)	14.463(5)	10.4128(6)	10.3922(10)	15.1171(2)	27.7139(13)
α /°	90	90	90	97.407(7)	90	90
β /°	102.351(7)	94.07(4)	96.868(5)	102.771(10)	90	90
γ /°	90	90	90	103.708(8)	90	90
V /Å^3	4061.1(6)	1273.2(7)	1614.6(2)	874.24(16)	4290.93(11)	8792.1(9)
Z	8	4	4	2	4	8
ρ_{calcd} /g·cm^{-3}	1.616	1.561	2.030	1.345	1.424	1.367
μ /cm^{-1}	10.703	1.374	1.395	1.896	1.968	2.455
Refl. meas./unique	5609/3305	3382/1509	6219/3114	5667/3359	10973/5787	23335/8584
Parameters refined	275	88	204	206	530	382
R_1, wR_2 (all)	0.0756, 0.1903	0.1951, 0.2323	0.1052, 0.2934	0.1004, 0.2140	0.0293, 0.0724	0.1585, 0.3815
R_1, wR_2 (obs)	0.0625, 0.1625	0.0912, 0.1859	0.0837, 0.2479	0.0639, 0.1756	0.0283, 0.0716	0.1289, 0.3460
Goodness of Fit	1.083	1.100	1.050	1.022	1.051	1.414

an appropriate metal salt and acetylenedicarboxylic acid (H_2ADC). Using methanolic solutions this yielded $Mn_2(ADC)_2(MeOH)_5$ (**MnADC**) and $Co(ADC)(MeOH)_4$ (**CoADC**). Difficulties were encountered growing single crystals of Zn containing phases using methanol as a solvent, therefore this was replaced with ethanol. $Zn_2(ADC)_3(HHUN)_3(NO_3)$ (**ZnADC1**) was made using a similar vapor diffusion approach to **MnADC** and **CoADC** while $Zn_3(ADC)_4(HHUN)_2$ (**ZnADC2**) was synthesized using a layered reaction. Vapor diffusion techniques were unsuccessful for making Ni-containing acetylenedicarboxylate coordination frameworks but layering techniques yield $Ni(ADC)(MeOH)(EtOH)_3$ (**NiADC1**) and $Ni(ADC)(EtOH)_4$ (**NiADC2**) from ethanolic solutions. The crystallographic details for these six compounds are presented in Table 1.

MnADC adopts a complex monoclinic structure with *C*2/*c* symmetry. The asymmetric unit of **MnADC** consists of three manganese sites (two of which lie on special positions with half the multiplicity of the general position), two ADC ligands and five methanol groups, all coordinated to the metal centers (see Figure 1). The structure is most simply thought of as containing planes comprising one of the three distinct cation types perpendicular to the *c*-axis, alternating in the sequence Mn1–Mn3–Mn2–Mn3–Mn1 (see Figure 2). There is no direct connectivity of the octahedra within such planes with connectivity along the *a* and *b* axes between octahedra of different types through carboxylate groups instead. Along the *c* axis connectivity occurs through both carboxylate groups and the backbone of the ligand. Overall this gives the structure $\mathbf{I^0O^3}$ connectivity by the nomenclature of *Cheetham* et al.[28]

All Mn cations are in octahedral environments but differ in the ligands coordinated to the metals. Mn1 and Mn2 are coordinated to four ADC linkers and two methanol ligands, the latter arranged in *trans*- and *cis* positions for Mn 1 and Mn2, respectively. Mn3, in contrast is coordinated to three ADC linkers and three methanol ligands, in a *mer*-configuration. They also vary in their degree of distortion with Mn3 being most ideal and Mn1 and Mn2 having significantly more deviation from an ideal octahedra with regards to bond lengths and bond angles, respectively (see Tables S1 and S2, Supporting Information). The bond valence sums are 1.92, 1.98 and 1.99 for Mn1, Mn2 and Mn3, respectively, consistent with that expected for divalent Mn.[29] Each methanol ligand is only coordinated to one cation but three of the four carboxylate groups from the two distinct ADC ligands have both of their oxygen atoms coordinated to a Mn. The only carboxylate oxygen atom that is not coordinated to a transition metal, O2, is involved in moderate hydrogen bonds with the hydrogen atom of the alcohol groups of two methanol ligands, with donor–acceptor (D–A) distances of 2.686(12) and 2.735(10) Å. The alcohol groups of the other three methanol ligands form two-center hydrogen bonds with coordinated oxygen atoms from three distinct carboxylate groups; these have D-A distances of 2.733(6), 2.776(9), and 2.818(7) Å.

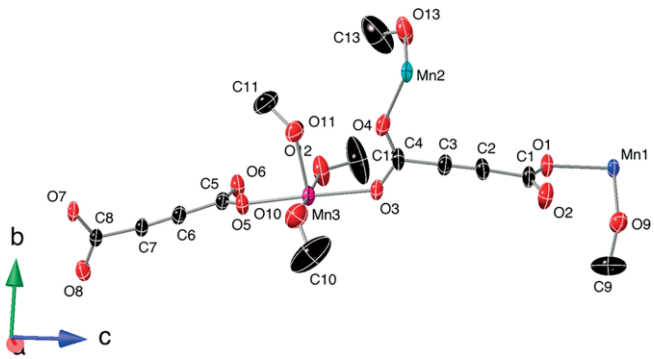

Figure 1. Depiction of the asymmetric unit of **MnADC** with atoms shown as thermal ellipsoids with 40 % probability distribution. Mn1, Mn2 and Mn3 are shown as dark blue, cyan and pink spheres, respectively, with carbon and oxygen atoms in black and red. Hydrogen atoms are omitted for clarity.

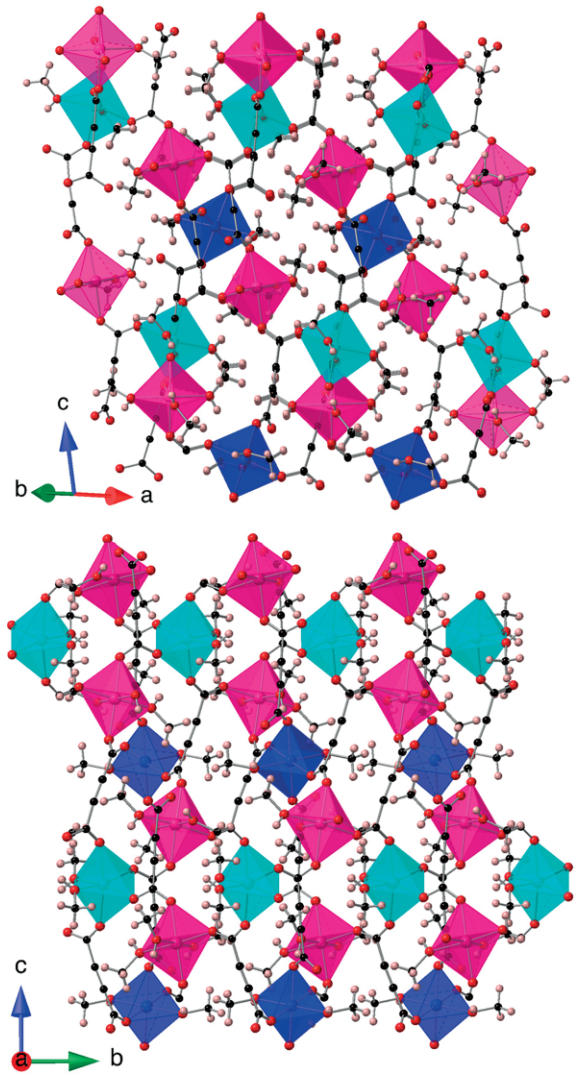

Figure 2. Depictions of **MnADC**. Mn1, Mn2 and Mn3 are shown in dark blue, cyan and pink, respectively, with carbon, hydrogen and oxygen atoms in black, pink and red.

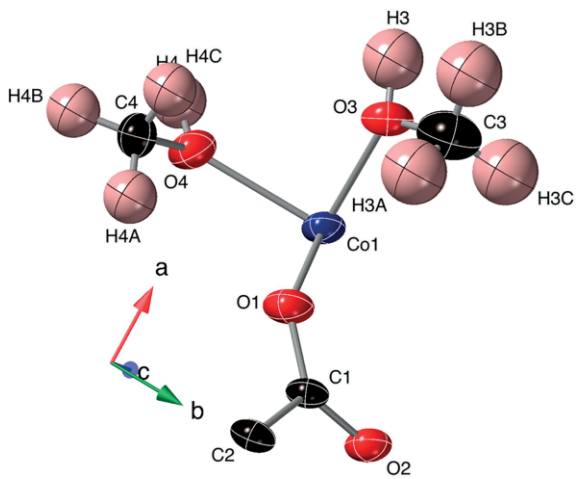

Figure 3. Depiction of the asymmetric unit of **CoADC** with atoms shown as thermal ellipsoids with 40% probability distribution. Co atoms are shown in dark blue with all other colors as in Figure 2.

CoADC adopts monoclinic *C*2/*c* symmetry. The asymmetric unit has one Co site, which lies on a special position with half the occupancy of the general position, half of an ADC linker and two coordinated solvent molecules (see Figure 3). The CoO_6 octahedra are close to ideal (see Tables S1 and S2, Supporting Information) and are connected to each other via the ADC linkers along the [101] direction with only weak intermolecular interactions holding the structure together in other directions, leading to $\mathbf{I^0O^1}$ connectivity (see Figure 4).[28] Neighboring chains are shifted by half a unit cell length along the *b*-axis. Overall this forms a dense framework with no useful porosity. Each methanol and carboxylate group on the ligands is only coordinated to one metal. The uncoordinated carboxylate group oxygen atom forms a hydrogen bond with both of the two distinct methanol alcohol groups with ^{d}–A distances of 2.687(6) and 2.704(9) Å. Each cation is coordinated to six oxygen atoms, the four equatorial sites being occupied by co-

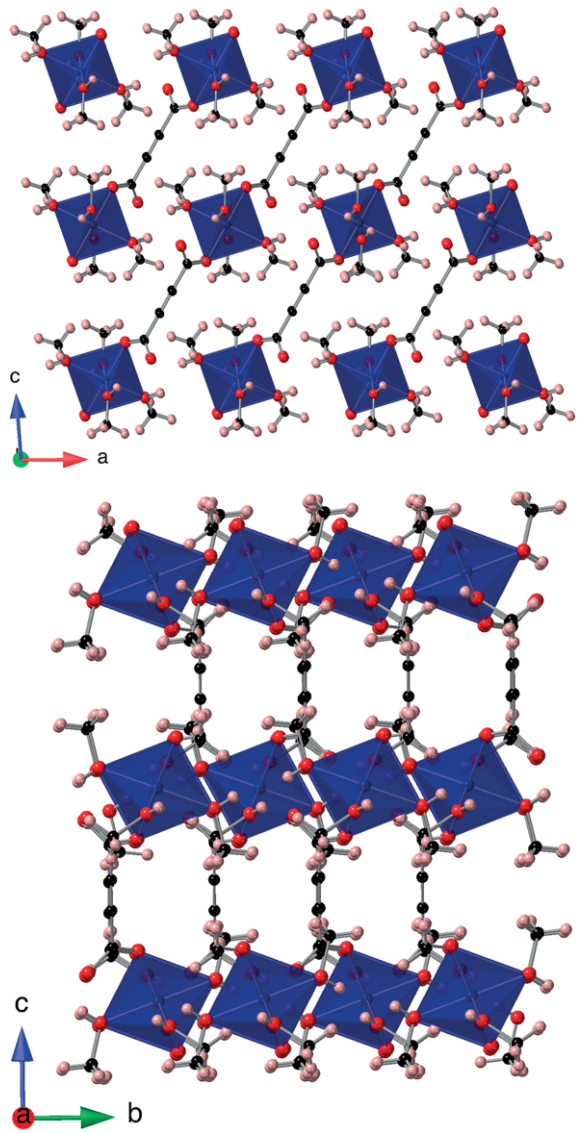

Figure 4. Depictions of **CoADC** with the Co cations shown in dark blue and all other atoms depicted as in Figure 2.

ordinated methanol and the axial sites by the ADC linker. The Co bond valence is 2.07, consistent with the presence of Co^{2+}.[29]

NiADC1 and **NiADC2** have $P2_1/n$ monoclinic and $P\bar{1}$ triclinic symmetry, respectively. They adopt similar structures in which octahedra Ni cations are linked into chains by the ADC ligand into structures with $\mathbf{I^0O^1}$ connectivity (see Figure 5 and Figure S1, Supporting Information).[28] The octahedra are closely packed in one orthogonal direction but are well separated in the other, with the coordinated methanol and ethanol ligands oriented in this direction. This leads to what appears to be a layered structure despite the lack of covalent bonding in one direction within the layers. The largest difference between the structures of these materials, aside from the coordinated solvents, is that in **NiADC1** the polyhedra are shifted half a unit cell along the [101] axis resulting in an ABAB stacking of these layers. In contrast the octahedra in **NiADC2** lack this offset, although the lower symmetry of this structure means that octahedra in adjacent layers do not lie directly on top of each other.

The asymmetric units of **NiADC1** and **NiADC2** are similar containing one Ni cation and one ADC ligand but differ in that **NiADC1** contains three ethanol ligands and one methanol ligand while **NiADC2** has four ethanol ligands (see Figure S2, Supporting Information). The alcohol ligands are somewhat disordered with one ethanol ligand in **NiADC1** split over two positions while the oxygen from another is also disordered while three of the four ethanol ligands in **NiADC2** have some degree of disorder. The Ni polyhedra are moderately distorted (see Tables S1) and in both compounds have ADC ligands coordinated in the *trans*-position with the three ethanol ligands in a *mer*-arrangement in **NiADC2**. The Ni cations in **NiADC1** and **NiADC2** have bond valence sums of 1.99 and 2.04, consistent with divalent cations.[29] Each of the carboxylate groups in the one unique ADC ligand in each structure coordinates to one cation through one of their oxygen atoms. In both structures the two uncoordinated oxygen atoms from the carboxylate groups of the ADC ligands are involved in two hydrogen bonds each; these hydrogen bonds are very similar in length in both materials with those in **NiADC1** having D–A distances between 2.541(7) and 2.713(8) Å while in **NiADC2** the D–A distances vary from 2.573(5) and 2.716(11) Å.

ZnADC1 adopts $Pna2_1$ orthorhombic symmetry, with an asymmetric unit containing two Zn atoms, four ADC ligands, three HHUN and a NO_3^- anion (see Figure 6). The Zn cations and ADC ligands are assembled into a wine-rack framework, with $\mathbf{I^0O^3}$ connectivity,[28] built around paddlewheel Zn dimers. The typical four carboxylate groups connect Zn within a dimer and the fifth site of each Zn coordinated to oxygen atom from a carboxylate group that only binds to one metal

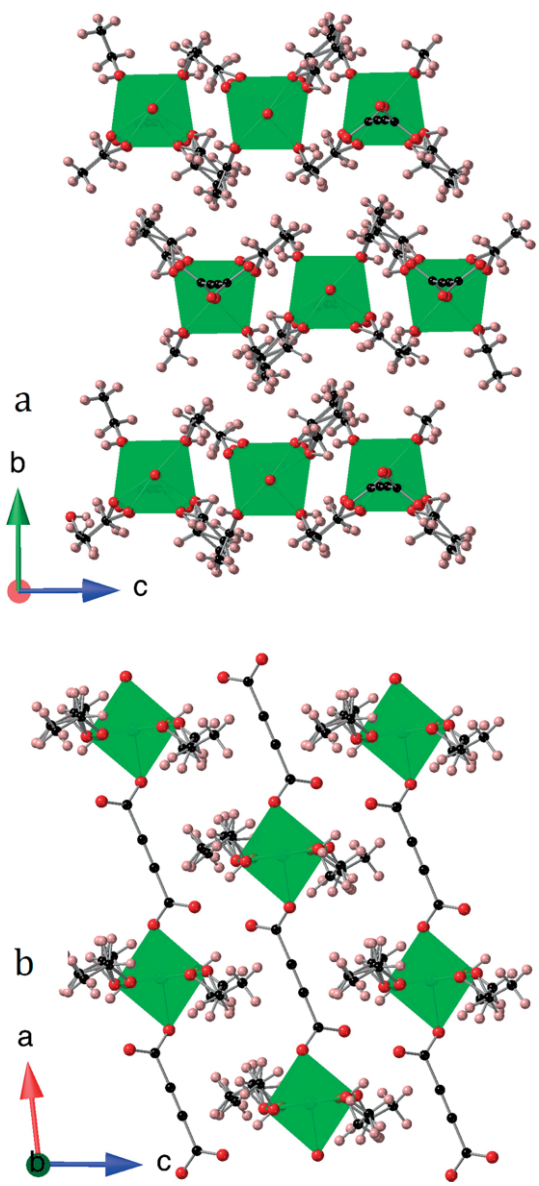

Figure 5. Depictions of **NiADC1** showing a) the stacking of the apparent layers in this structure and b) the structure of an individual apparent layer. Ni cations are shown in light green and all other atoms depicted as in Figure 2.

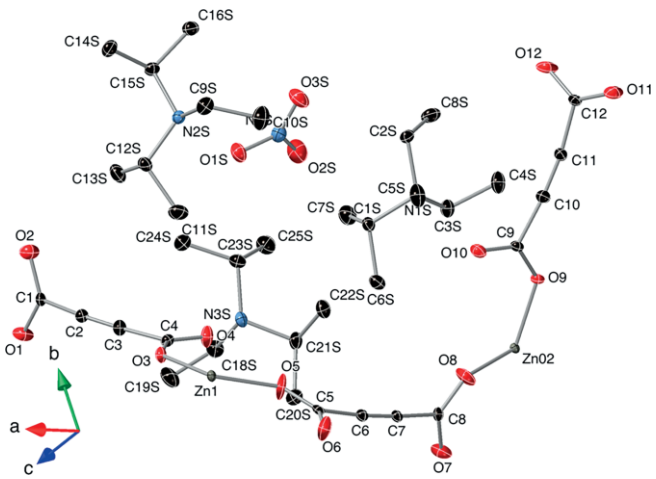

Figure 6. Depiction of the asymmetric unit of **ZnADC1** with atoms shown as thermal ellipsoids with 40 % probability distribution. Zn atoms are shown in grey and N in blue with all other atoms are depicted in Figure 1. Hydrogen atoms are omitted for clarity.

(see Figure 7). Such dimers are a common secondary building unit in MOFs incorporating either Cu or Zn combined with rigid, typically aromatic, carboxylate ligands, including the archetypical HKUST-1.[30–32] The square pyramidal Zn are slightly distorted, with a shortened axial Zn–O bond (see Tables S1 and S2, Supporting Information). The bond valence sums of the Zn cation are 2.13 and 2.09, consistent with the presence of Zn^{2+}.[29] The ADC ligand bridges dimers along the <100> and <011> directions, with the orientation of the dimers rotating 90° compared to their neighbors along the *a*-axis. The two ADC ligands connecting dimers within the *bc* plane connect to three distinct metals each through three of their four carboxylate oxygen atoms while the ADC ligand providing connectivity along the *a*-axis coordinates to four distinct metals through their four carboxylate oxygen atoms. The two uncoordinated oxygen atoms in the carboxylate ligand both form a hydrogen bond with the hydrogen bonded to the amine in a HHUN cation, with D–A distances of 2.805(4) and 2.817(4) Å.

Overall the $[Zn_2(ADC)_3]^{2-}$ charge of the anionic framework is balanced by the occupation of the pore by a HHUN with its nitrogen atom in the center of each pore window and a NO_3^- anion in the center of the pore; the remaining significant hydrogen bond in the structure is formed between the hydrogen bonded to the nitrogen in the third HHUN cation to one of the oxygen atoms in the NO_3^- anion with a D–A distance of 2.817(4) Å. This leads to the structure not having any significant useable porosity in the absence of a method for removing the counterions while retaining charge balance; if this could be achieved then void calculations in Mercury 4.0[33] indicates 69.6 % of the structure would be empty pore space accessible by a probe with a 1.2 Å radius, the van der Waals radius of hydrogen.

ZnADC2 adopts *Pbca* orthorhombic symmetry, with an asymmetric unit comprised of three Zn sites, four ADC linkers and two HHUN molecules (see Figure 8). The nodes in the material are comprised of a central octahedral Zn, which is linked by opposite corners to two distinct tetrahedral Zn cations (see Figure 9). Each node is connected through six ADC linkers to six neighboring nodes rotated from each other by 90°. Only one linker connects nodes within the *ac* plane but two along the *b*-axis. Overall, this leads to a $\mathbf{I^0O^3}$ framework structure with oval channels running along the *b*-axis.[28] The channels are partially occupied by HHUN molecules, with two of these for each cavity bordered by eight nodes, with the HHUN molecules displaced from the center of the cavities along the *a*-axis. Void calculations using Mercury 4.0[33] with a 1.2 Å radius probe suggests an empty pore volume of 13.5 % in the framework, running continuously along the center of the pores, which in principal increases to 58.2 % if the pores could be emptied while retaining charge balance. With the counter cations in the pores increasing the probe to the van der Waals radius of any halides leads to isolated voids, suggesting that it will be difficult for such gases to enter the structure.

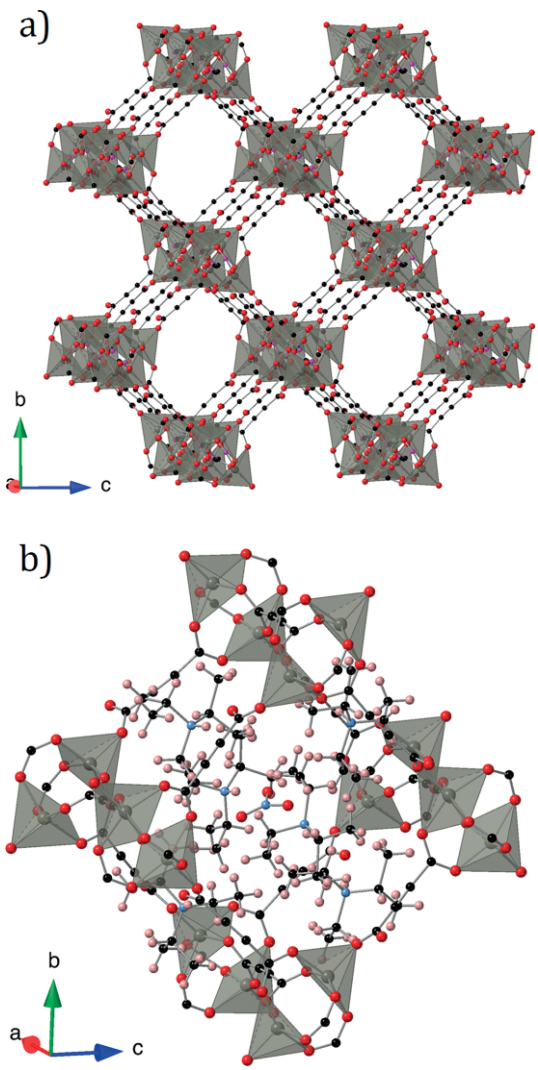

Figure 7. Depictions of the structure of **ZnADC1** showing (a) the framework with the contents of the pore omitted and (b) one cage of the framework including the HHUN and NO_3^- ions in its pores. Zn atoms are shown in grey and N in blue and all other atoms are depicted in the colors shown in Figure 2.

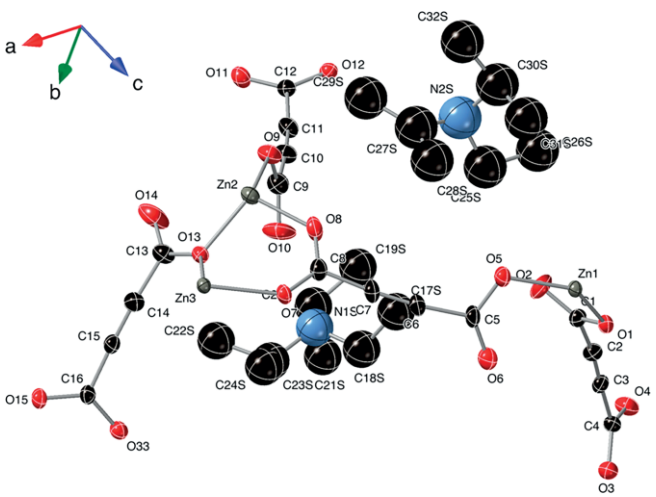

Figure 8. Depiction of the asymmetric unit of **ZnADC2** with atoms shown as thermal ellipsoids with 40 % probability distribution. Zn atoms are shown in grey and N in blue and all other atoms are depicted as shown in Figure 1. Hydrogen atoms are omitted for clarity.

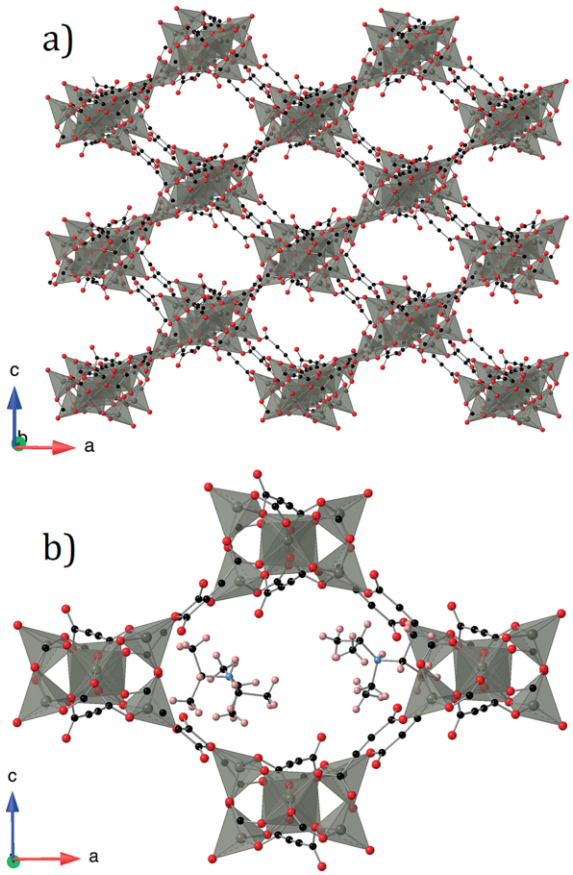

Figure 9. Depictions of the structure of **ZnADC2** showing (a) the framework with the contents of the pore omitted and (b) one cage of the framework including the HHUN ions in its pores. Zn atoms are shown in grey and N in blue and all other atoms are depicted in the colors shown in Figure 2.

The Zn cations are coordinated to only one oxygen atom from either four or six different ADC linkers while all ADC linkers are coordinated to three Zn cations through three oxygen atoms from their carboxylate groups. Only one of the HHUN cations in the pores of the framework is involved in a hydrogen bond with the framework, specifically one of the uncoordinated carboxylate oxygen atoms with a D–A distance of 3.01(2) Å. This is much longer than the other hydrogen bonds reported in this study, including **ZnADC1**, and the weaker hydrogen bonding in **ZnADC2** may play a role in the larger displacement parameters of the HHUN cations in this material compared to **ZnADC1**. The lack of hydrogen bonds to stabilize the uncoordinated carboxylate oxygen atoms in this structure appears to be compensated by these having somewhat shorter C–O bond lengths; these vary between 1.214(11) and 1.226(10) Å, compared to other carboxylate C–O distances in the structure, which vary between 1.209(12) Å (which is associated with the uncoordinated carboxylate oxygen atom involved in hydrogen bonding) and 1.302(10) Å. The Zn coordination environments are moderately distorted from ideal geometry, primarily due to distortions in bond angles for the tetrahedral environments and bond lengths in the octahedra (see Tables S1 and S2, Supporting Information). The bond valence sums are 1.97 for both tetrahedral cations and 2.13 for the octahedral Zn.[29]

The common trend across all structures determined in this work having at least some carboxylate groups that only coordinate through one of their two oxygen atoms is consistent with other reported ADC coordination polymers, including $M(ADC)(H_2O)_2$ (M = Mn, Co, Ni, and Zn),[20,23–25] $M(ADC)(H_2O)_4{\cdot}2H_2O$ (M = Co and Ni),[23,25] $M(ADC)(CH_3)_2NCOH)_2(H_2O)_2$ (M = Mn, Co, Ni, and Zn),[34] $M(ADC)(C_5H_5N)_2(H_2O)_2$ (M = Fe, Co, Ni, and Zn)[26,27] and MOF-31, $Zn(ADC)_2{\cdot}(HN(CH_2CH_3)_3)_2$.[11] This is in contrast to many other linear dicarboxylate polymers where both oxygens in a carboxylate will coordinate to at least one metal. This is likely a reflection of the highly rigid nature of the ADC ligand making higher coordination of the carboxylate groups more difficult. In most structures reported in this work, with the exception of ZnADC2, all uncoordinated oxygen atoms in the ADC carboxylate groups exhibit one, and more commonly, two hydrogen bonds that help to stabilize these.

$M(ADC)(H_2O)_4{\cdot}2H_2O$,[23,25] $M(ADC)(((CH_3)_2NCOH)_2(H_2O)_2)$,[34] and $M(ADC)(C_5H_5N)_2(H_2O)_2$[26,27] have analogous chemical formula to the Co and Ni phases in this work, with all having four coordinated solvent molecules in equatorial positions. All of these materials are also 1D polymers, suggesting that other phases with similar composition would also likely be so. As can be seen, however, by a comparison of the structures of **CoADC**, **NiADC1** and **NiADC2**, however, within these 1D polymers there can be significant structural difference. **NiADC1** and **NiADC2** adopt very similar structures, despite their differences in symmetry, which vary only in **NiADC1** featuring one methanol and three ethanol co-ligands while **NiADC2** has only four ethanol co-ligands. Overall both their structures at first glance resemble layered compounds due to the co-ligands occupying the space between their layers, although there is only connectivity within one direction of these layers provided by the ADC ligand. In contrast **CoADC** adopts a structure in which its 1D nature is much more immediately visually apparent, possible because of only containing smaller methanol co-ligands, which reduce the steric bulk of the co-ligands. The more complex structure and composition of **MnADC** has no direct analogue with related ADC frameworks to the best of our knowledge.

The two 3D MOFs uncovered in this work both contain anionic frameworks comprised of Zn connected by ADC ligands with charge balance achieved by the counterions in their pores. Both of the two Zn MOFs reported thus far that only incorporate ADC as organic ligands are IRMOF-0,[10] which is isostructural with MOF-5, and MOF-31,[11] which adopts an augmented diamond topology, were also found to feature amines in their pores, specifically triethylamine. MOF-31, whose structure has been solved enabling its composition to be clearly determined, also has an anionic framework. This is charge balanced by protonated amine in its pores, triethylamine, similarly to HHUN in **ZnADC1** and **ZnADC2**. These guest molecules are unlikely to be readily removed from the framework as this would require a mechanism for these to be charged balanced.

IRMOF-0[10] is reported to have neutral triethylamine in its pores but thermogravimetric analysis indicates that the guests are not removed from the pores before the material and thus also cannot be removed. Despite the structural similarities often exhibited between Cu and Zn there are no known Cu compounds that only feature ADC ligands.

Bulk Characterization

Attempts were made to obtain powder X-ray diffraction patterns of compounds made in this work to enable further analysis but this was unsuccessful in most cases. **MnADC** and **CoADC** were found to rapidly decompose, likely due to solvent loss, to form $M(ADC)(H_2O)_2$ (M = Mn or Co) (see Figure S3, Supporting Information).[23,24] The powder diffraction pattern obtained from a bulk sample of **NiADC1** indicated this was poorly crystalline such that its identity could not be clearly be confirmed although it was broadly consistent with **NiADC1** being the bulk phase present (see Figure S4, Supporting Information). **NiADC2** was formed in trace quantities such that it was not possible to obtain sufficient sample of this material to obtain a powder X-ray diffraction pattern.

The powder X-ray diffraction pattern of **ZnADC1** indicated this was clearly the main phase present in the bulk and that it is likely more stable than the phases formed in this work (see Figure S5, Supporting Information). Additional weak peaks in the diffraction pattern, however, indicate that it was not possible to synthesize a pure sample of this material. The purity was, however, sufficient to enable further characterization of this sample. The infrared spectrum of this material was particularly useful as peaks associated with C-H and N-H groups are present that cannot be explained by the framework but, instead, indicate the presence of Hunig's base in the pores of this compound (see Figure S6, Supporting Information). Thermogravimetric analysis also indicated the material decomposed around 130 °C, predominantly via a single exothermic process (Figure S7, Supporting Information). This confirms that it is not possible to evacuate the pores of the material, consistent with it having been occupied by counter cation and anions rather than neutral guest molecules.

The powder X-ray diffraction pattern of a sample of **ZnADC2** indicated the bulk composition is primarily a mixture of **ZnADC2** and $Zn(ADC)(H_2O)_2$,[20] with the latter the dominant phase (see Figure S8, Supporting Information). Similar to **ZnADC1** peaks in the infrared spectrum of this material supported the presence of Hunig's base in the pores of this compound (see Figure S9, Supporting Information).

Conclusions

This work reports the synthesis and crystal structures of six new transitions metal coordination polymers incorporating the acetylenedicarboxylate ligand, all made at ambient temperatures. Three of these materials, **CoADC**, **NiADC1** and **NiADC2**, are 1D coordination polymers while 3D **MnADC**, **ZnADC1** and **ZnADC2** can be considered MOFs. Of these **ZnADC1** and **ZnADC2** contain significant potential pore space but the ability to access this is greatly reduced by the presence of ions in the pores of these materials, which are required to charge balance their anionic frameworks. The ability to study these compounds in any form is greatly reduced by the instability of the Mn, Co and Ni phases once they are removed from solution, most likely due to solvent loss. The Zn containing phases are more robust allowing the use of IR spectroscopy to confirm the presence of protonated base in their pores. For **ZnADC1**, which is obtained with high purity, TGA indicates this material decomposes in a single step when heated, highlighting the likely difficulty of emptying the pores of this material.

Experimental Section

MnADC: The compound was made using 5 mL of a methanol solution containing 0.2 M $Mn(NO_3)_2{\cdot}4H_2O$ and 0.3 M acetylenedicarboxylic acid with 8 mL of a 0.25 M *N*,N'-diisopropylethylamine, also known as Hunig's base (HUN), solution in methanol. This reaction was left undisturbed until crystals from these reactions formed, typically after between two to three weeks, which were then harvested for crystal structure determination.

CoADC: The compound was made using the same approach as **MnADC** but with $Mn(NO_3)_2{\cdot}4H_2O$ substituted for $CoCl_2{\cdot}4H_2O$.

ZnADC1: The compound was made using a 5 mL solution of 0.2 M $Zn(NO_3)_2{\cdot}6H_2O$ and 0.3 M ADC in ethanol and 8 mL of 0.25 M Hunig's base solution in ethanol. Crystals formed after 1 week suitable for crystal structure determination. A purer bulk phase of this sample was synthesized by changing the reagent concentrations to 0.22 M, 0.32 M and 0.26 M for $Zn(NO_3)_2{\cdot}6H_2O$, ADC and Hunig's base.

ZnADC2: The compound was synthesized using a layered reaction, comprising 5 mL of 0.2 M $Zn(NO_3)_2{\cdot}6H_2O$ in ethanol as a bottom layer, 5 mL of ethanol in the buffer layer and 8 mL of 0.3 M H_2ADC and 0.25 M Hunig's base in ethanol in the top layer. Crystals suitable for X-ray diffraction were harvested after 2 weeks.

NiADC1: The compound was made via a layered reaction using 5 mL ethanol solution containing 0.2 M $Ni(NO_3)_2{\cdot}6H_2O$ as a bottom layer, 5 mL of ethanol as a buffer layer and 5 mL of ethanol solution containing 0.3 M H_2ADC and 0.4 M triethylamine in the top layer. This reaction was left undisturbed until crystals formed, typically after 1 week.

NiADC2: The compound was made by a similar method to **NiADC1** but substituting ethanol for methanol as a solvent.

Crystal Structure Determination: Crystal structure determination was carried out using a dual source Rigaku Oxford Diffraction Supernova equipped with Mo-K_α and Cu-K_α micro-focus sources (50 kV, 0.8 mA) with multi-layered optics and an Atlas S2 CCD detector. Samples were either analysed at ambient temperature or cooled and ran at 100 K using an Oxford Cryosystems cryostream with samples held on MiTeGen microloops. Data were integrated and absorption correction performed using the CrysAlisPro software suite.[35] Structures were solved by direct methods in SHELXT[36] or charge flipping methods in olex.2,[37] with least-squares refinements carried out using SHELXL-2014[38] via the Olex2 graphical user interface.[39] Typically displacement parameters of non-hydrogen atoms were refined anisotropically and hydrogen atom position located geometrically using the AFIX commands in SHELX-2014,[38] with their displacement parameters constrained to 1.2 or 1.5 times the carbon or oxygen atoms they were

connected to, respectively (see Table 1 for crystallographic details). A noticeably worse fit was obtained to the data obtained from **ZnADC2** compared to the other structures obtained in this fit; this is a result of residual disordered electron density in the pores of this crystal structure. This can be accounted for by the use SQUEEZE programme[40] but this prevents stable modeling of the HHUN cations that can be clearly seen in the pores of this framework.

Crystallographic data (excluding structure factors) for the structures in this paper have been deposited with the Cambridge Crystallographic Data Centre, CCDC, 12 Union Road, Cambridge CB21EZ, UK. Copies of the data can be obtained free of charge on quoting the depository numbers CCDC-2016275, CCDC-2016276, CCDC-2016277, CCDC-2016278, CCDC-2016279, and CCDC-2016280 (Fax: +44-1223-336-033; E-Mail: deposit@ccdc.cam.ac.uk, http://www.ccdc.cam.ac.uk).

Bulk Phase Analysis: Bulk phase analyses were carried out using a Rigaku Miniflex powder X-ray diffractometer using Cu-K_α radiation (40 kV, 15 mA) and a D/tex Ultra detector with samples held on zero background plates and data collected over a range of 5–60° 2θ. Data was fitted using the LeBail method as implemented in the Rietica programme.[41] Thermal stability of **Zn1** was measured using a NETZSCH 409 PG/PC TGA with the sample held in an Al_2O_3 crucible and heated under flowing air at a rate of 10 K·min^{-1} over a 25 to 600 °C range. Infrared spectra were collected over a range of 500–4000 cm^{-1} using a Shimadzu IRAffinity-1S Fourier transform spectrometer equipped with an attenuated total reflection stage. Measurements were averaged over a total of 16 scans.

Supporting Information (see footnote on the first page of this article): Further crystal structure images and details, powder X-ray diffraction patterns, infrared spectra and thermal analysis can be seen in the supporting information.

Acknowledgements

We would like to thank the University of Kent for supporting this work.

Keywords: Metal-organic frameworks; Acetylenedicarboxylate; Coordination polymer; Transition metals

References

[1] S. R. Batten, N. R. Champness, X.-M. Chen, J. Garcia-Martinez, S. Kitagawa, L. Öhrström, M. O'Keeffe, M. P. Suh, J. Reedijk, *CrystEngComm* **2012**, *14*, 3001–3004.
[2] S. Seth, A. J. Matzger, *Cryst. Growth Des.* **2017**, *17*, 4043–4048.
[3] A. J. Howarth, A. W. Peters, N. A. Vermeulen, T. C. Wang, J. T. Hupp, O. K. Farha, *Chem. Mater.* **2017**, *29*, 26–39.
[4] C. N. R. Rao, A. K. Cheetham, A. Thirumurugan, *J. Phys. Condens. Matter* **2008**, *20*, 83202.
[5] H. Furukawa, K. E. Cordova, M. O'Keeffe, O. M. Yaghi, *Science* **2013**, *341*, 1230444.
[6] P. Ramaswamy, N. E. Wong, G. K. H. Shimizu, *Chem. Soc. Rev.* **2014**, *43*, 5913–5932.
[7] W. Li, Z. Wang, F. Deschler, S. Gao, R. H. Friend, A. K. Cheetham, *Nat. Rev. Mater.* **2017**, *2*, 16099.
[8] P. J. Saines, N. C. Bristowe, *Dalton Trans.* **2018**, *47*, 13257–13280.
[9] A. Airi, C. Atzori, F. Bonino, A. Damin, S. Øien-Ødegaard, E. Aunan, S. Bordiga, *Dalton Trans.* **2020**, *49*, 12–16.
[10] D. J. Tranchemontagne, J. R. Hunt, O. M. Yaghi, *Tetrahedron* **2008**, *64*, 8553–8557.
[11] J. Kim, B. Chen, T. M. Reineke, H. Li, M. Eddaoudi, D. B. Moler, M. O'Keeffe, O. M. Yaghi, *J. Am. Chem. Soc.* **2001**, *123*, 8239–8247.
[12] Y.-Q. Zheng, J. Zhang, J.-Y. Liu, *CrystEngComm* **2010**, *12*, 2740–2748.
[13] T. J. M. Ma Ntep, H. Reinsch, B. Moll, E. Hastürk, S. Gökpinar, H. Breitzke, C. Schlüsener, L. Schmolke, G. Buntkowsky, C. Janiak, *Chem. Eur. J.* **2018**, *24*, 14048–14053.
[14] T. J. Matemb Ma Ntep, H. Reinsch, C. Schlüsener, A. Goldman, H. Breitzke, B. Moll, L. Schmolke, G. Buntkowsky, C. Janiak, *Inorg. Chem.* **2019**, *58*, 10965–10973.
[15] D. Tiana, C. H. Hendon, A. Walsh, *Chem. Commun.* **2014**, *50*, 13990–13993.
[16] R. J. Marshall, T. Richards, C. L. Hobday, C. F. Murphie, C. Wilson, S. A. Moggach, T. D. Bennett, R. S. Forgan, *Dalton Trans.* **2016**, *45*, 4132–4135.
[17] R. J. Marshall, S. L. Griffin, C. Wilson, R. S. Forgan, *J. Am. Chem. Soc.* **2015**, *137*, 9527–9530.
[18] R. J. Marshall, S. L. Griffin, C. Wilson, R. S. Forgan, *Chem. Eur. J.* **2016**, *22*, 4870–4877.
[19] J. Li, T. B. Brill, *J. Phys. Chem. A* **2002**, *106*, 9491–9498.
[20] I. Stein, U. Ruschewitz, *Acta Crystallogr., Sect. E* **2005**, *61*, m2680–m2682.
[21] S. Skoulika, P. Dallas, M. G. Siskos, Y. Deligiannakis, A. Michaelides, *Chem. Mater.* **2003**, *15*, 4576–4582.
[22] H. Billetter, F. Hohn, I. Pantenburg, U. Ruschewitz, *Acta Crystallogr., Sect. C* **2003**, *59*, m130–m131.
[23] I. Pantenburg, U. Ruschewitz, *Z. Anorg. Allg. Chem.* **2002**, *628*, 1697–1702.
[24] C. Robl, S. Hentschel, *Z. Anorg. Allg. Chem.* **1990**, *591*, 188–194.
[25] F. Hohn, H. Billetter, I. Pantenburg, U. Ruschewitz, *Z. Naturforsch. B* **2002**, *57*, 1375–1381.
[26] I. Stein, M. Speldrich, H. Schilder, H. Lueken, U. Ruschewitz, *Z. Anorg. Allg. Chem.* **2007**, *633*, 1382–1390.
[27] I. Stein, U. Ruschewitz, *Z. Naturforsch. B* **2009**, *64*, 1093–1097.
[28] A. K. Cheetham, C. N. R. Rao, R. K. Feller, *Chem. Commun.* **2006**, 4780–4795.
[29] N. E. Brese, M. O'Keeffe, *Acta Crystallogr., Sect. B* **1991**, *47*, 192–197.
[30] S. Vagin, A. K. Ott, B. Rieger, *Chem. Ing. Technol.* **2007**, *79*, 767–780.
[31] S. S.-Y. Chui, S. M.-F. Lo, J. P. H. Charmant, A. G. Orpen, I. D. Williams, *Science* **1999**, *283*, 1148–1150.
[32] M. Edgar, R. Mitchell, A. M. Z. Slawin, P. Lightfoot, P. A. Wright, *Chem. Eur. J.* **2001**, *7*, 5168–5175.
[33] C. F. Macrae, I. Sovago, S. J. Cottrell, P. T. A. Galek, P. McCabe, E. Pidcock, M. Platings, G. P. Shields, J. S. Stevens, M. Towler, P. A. Wood, *J. Appl. Crystallogr.* **2020**, *53*, 226–235.
[34] D. Hermann, C. Näther, U. Ruschewitz, *Solid State Sci.* **2011**, *13*, 1096–1101.
[35] CrysAlis PRO, version 171.38.43, Rigaku Oxford Diffraction, **2018**.
[36] G. M. Sheldrick, *Acta Crystallogr., Sect. A* **2015**, *71*, 3–8.
[37] L. J. Bourhis, O. V. Dolomanov, R. J. Gildea, J. A. K. Howard, H. Puschmann, *Acta Crystallogr., Sect. A* **2015**, *71*, 59–75.
[38] G. M. Sheldrick, *Acta Crystallogr., Sect. C* **2015**, *71*, 3–8.
[39] O. V. Dolomanov, L. J. Bourhis, R. J. Gildea, J. A. K. Howard, H. Puschmann, *J. Appl. Crystallogr.* **2009**, *42*, 339–341.
[40] A. L. Spek, *Acta Crystallogr., Sect. C* **2015**, *71*, 9–18.
[41] B. A. Hunter, C. J. Howard, A Computer Program for Rietveld Analysis of X-ray and Neutron Powder Diffraction Patterns, **1998**.

Received: July 16, 2020
Published Online: September 14, 2020